Contract No:

This document was prepared in conjunction with work accomplished under Contract No. 89303321CEM000080 with the U.S. Department of Energy (DOE) Office of Environmental Management (EM).

Disclaimer:

Integrated Fuel Cycle Materials and Chemistry Program: FY21 Plutonium Science Task Report

Jonathan H. Christian

Eliel Villa-Aleman

Amy Hixon

Bryan J. Foley

Elodia Ciprian

Don D. Dick

September 2021

SRNL-STI-2021-00371, Revision 0

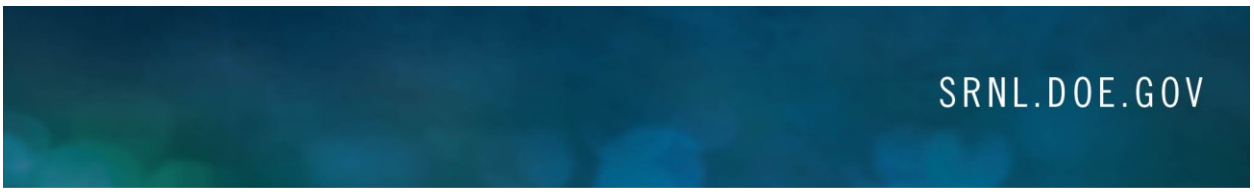

DISCLAIMER

Printed in the United States of America

Prepared for
U.S. Department of Energy

SRNL-STI-2021-00371
Revision 0

Keywords: *plutonium, fuel cycle, oxalate, fluoride, spectroscopy, diffraction*

Retention: *Varies*

Integrated Fuel Cycle Materials and Chemistry Program: FY21 Plutonium Science Task Report

Jonathan H. Christian
Eliel Villa-Aleman
Amy Hixon
Bryan J. Foley
Elodia Ciprian
Don D. Dick

September 2021

Savannah River National Laboratory is operated by Battelle Savannah River Alliance for the U.S. Department of Energy under Contract No. 89303321CEM000080.

PREFACE

The work described herein was executed in fiscal year 2021 as part of the NA-22 Integrated Fuel Cycle Materials and Chemistry Program.

EXECUTIVE SUMMARY

In fiscal year 2021 (FY21), the Integrated Fuel Cycle Materials and Chemistry Program (IFCMCP) executed numerous tasks related to Task 2, Plutonium Science, including:

- Production and extensive characterization of plutonium (IV) oxalate and its thermal degradation products
    - A manuscript on this work was submitted to Journal of Nuclear Materials (September 2021)
- Production and vibrational spectroscopy characterization of plutonium (IV) nitrate and plutonium (IV) fluoride hydrate.
- Shipment of 325 mg of weapons-grade plutonium dioxide from Savannah River National Laboratory (SRNL) to University of Notre Dame (UND)
- Development of gas-free synthetic methods to produce high-quality anhydrous actinide fluoride samples for use in subsequent characterization measurements.
- Analysis of the relationship between production parameters and physical properties for plutonium (IV) fluoride hydrate produced via aqueous precipitation.
- Graduation of the first UND graduate student supported under this program via the Oak Ridge Fuel Cycle Science Fellowship
- Appointment of the second UND graduate student to be supported under this program via the Oak Ridge Fuel Cycle Science Fellowship.
- Design and fabrication of next-generation spectroscopy containment cells for future experiments involving multiphoton ionization, laser ablation, and liquid analysis.

In this document, FY21 research results are discussed in detail and relevant background information is provided where necessary.

TABLE OF CONTENTS

LIST OF TABLES

LIST OF FIGURES

LIST OF ABBREVIATIONS

DRIFTS	Diffuse Reflectance Infrared Fourier Transform Spectroscopy
FY20	Fiscal Year 2020 (October 1, 2019 – September 30, 2020)
FY21	Fiscal Year 2021 (October 1, 2020 – September 30, 2021)
IFCMCP	Integrated Fuel Cycle Materials and Chemistry Program
IR	Infrared
SEM	Scanning Electron Microscopy
SRNL	Savannah River National Laboratory
TGA	Thermogravimetric Analysis
UND	University of Notre Dame
pXRD	Powder X-ray Diffraction

1.0 Introduction

Task 2 of the IFCMCP was designed to utilize vibrational spectroscopy, microscopy, X-ray diffraction, and calorimetry to explore the spectroscopic, structural, and chemical properties of plutonium compounds relevant to the nuclear fuel cycle. An important precursor to this work is production of fresh, high-quality plutonium samples. Given the health hazards and material accountability associated with plutonium, sample production is not trivial and production experiments require extensive planning and coordination by research and support staff. Further, because alpha-emissions from plutonium produce time- and dose-dependent radiolysis resulting in structural defects, particularly in the presence of water, freshly prepared plutonium samples must be carefully packaged and analyzed with urgency following their production.

In FY21, SRNL and UND engaged in numerous research studies involving production and subsequent characterization of plutonium dioxide, plutonium fluoride, plutonium oxalate, and plutonium nitrate. Specific efforts involving each of these compounds are described in detail below.

2.0 FY21 Progress on Specific Compounds

2.1 Plutonium (IV) Oxalate to Plutonium Dioxide

2.1.1 Background

Conversion of plutonium (IV) oxalate ($Pu(C_2O_4)_2$) to plutonium dioxide (PuO_2) via high-temperature calcination – a process commonly referred to as the Pu(IV) oxalate method - has been utilized for plutonium processing since the 1940s.[1] Due to its simplicity and dependability, the Pu(IV) oxalate method remains the standard for producing PuO_2 at industrial-scale nuclear fuel reprocessing facilities.[2] Despite the enduring utility of this method, and the numerous reports written about it, uncertainty abounds regarding the chemicophysical changes that occur during thermal decomposition of $Pu(C_2O_4)_2$. In fact, there are at least 8 different reports in the literature whose titles contain both the terms “thermal decomposition” and “plutonium (IV) oxalate”.

While these reports vary in their details, several consistencies have been established. First, Pu(IV) oxalate hexahydrate ($Pu(C_2O_4)_2•6H_2O$) is the chemical species formed when oxalic acid is mixed with an acidic plutonium (IV) nitrate solution; a result clearly established by powder X-ray diffraction (pXRD) analysis.[3] Second, heating $Pu(C_2O_4)_2•6H_2O$ causes dehydration to the plutonium (IV) oxalate dihydrate ($Pu(C_2O_4)_2•2H_2O$) and eventually anhydrous $Pu(C_2O_4)_2$.[3b, 4] Third, isolation of either anhydrous or monohydrate complexes of Pu(IV) oxalate is difficult due to their hygroscopic nature.[4] Fourth, the oxalate ligand decomposes with sufficient heating, eventually leading to the formation of PuO_2.[5]

Exact chemical structures of species formed as the oxalate ligand decomposes is an area of uncertainty that still surrounds $Pu(C_2O_4)_2•xH_2O$ degradation. The most informative descriptions on this topic have derived structural details from geometrically-optimized computational models that, with the exception of $Pu(C_2O_4)_2•6H_2O$ and $Pu(C_2O_4)_2•2H_2O$ which have published powder XRD patterns, have not been experimentally verified.[3, 6] In fact, a 2021 density functional theory (DFT) study of $Pu(C_2O_4)_2$ decomposition clearly states that the precise structural modifications occurring during thermal decomposition of $Pu(C_2O_4)_2$ have not been experimentally characterized, but *the DFT-derived intermediate structures should be identifiable using spectroscopy techniques*.[6a]

With this in mind, our team executed high-resolution Raman and IR spectroscopy measurements on $Pu(C_2O_4)_2•6H_2O$ and its degradation products that form up to 450 °C in air. Our experimental setup allowed for collection of high-resolution infrared data under an inert atmosphere using Diffuse Reflectance Infrared Fourier Transform Spectroscopy (DRIFTS) for the Pu-bearing compounds in a double-walled cell. The DRIFTS approach obviates the need for nujol, epoxy resins, or other protective coatings for analyzed specimens. The same material was also analyzed with Raman spectroscopy as Raman spectroscopy is a complementary technique to DRIFTS. The vibrational spectra presented herein provide details of

fundamental importance for these crucial nuclear fuel cycle compounds and can be used in future studies to verify the accuracy of theoretically-derived chemical structures. Considering the ubiquity of the Pu(IV) oxalate method in the nuclear fuel cycle, we believe the publication of these vibrational spectra is long overdue.

2.1.2 Synthesis and Thermal Degradation

In a 20 mL scintillation vial, $Pu(NO_3)_4$ (2.1 mL; 0.1 M in 3 M HNO_3; 0.21 mmol) was added dropwise over five minutes to a stirring solution of oxalic acid dihydrate (4 mL; 0.12 M in water; 0.48 mmol, 2.3 eq.). This solution was stirred for two hours during which time tan/dark white solids formed as expected for $Pu(C_2O_4)_2•6(H_2O)$; the solid composition was verified by pXRD (*vide infra)*. The suspension was gravity filtered through a filtration apparatus and dried under a positive pressure of argon for 2 hours. Removal of the filter membrane and collection of the tan solid yielded the product as a granular brown solid (See Fig. S1). Yield: 96 mg (87%).

Freshly prepared $Pu(C_2O_4)_2•6(H_2O)$ solid was divided into six glass vials; five of these were placed into a muffle furnace (Thermo Fisher FB1315M) to undergo heating within a negative pressure radiological glovebox. A heating program was then initiated on the furnace. When establishing a temperature, the furnace set point was set ca. 20 °C below the desired temperature to prevent the temperature of the furnace from exceeding the set point. After the temperature had stabilized, the set point of the furnace was moved to the desired temperature and held for one hour. After one hour, the oven was opened and a vial was removed. The furnace was then raised to the next temperature. This process was performed at 100, 220, 250, 350, and 450 °C. The removed samples were weighed and transferred into sealed glass vials for storage.

2.1.3 Characterization Results

The thermal decomposition of $Pu(C_2O_4)_2•6(H_2O)$ to PuO_2 was characterized with vibrational spectroscopy (Raman and infrared) and pXRD. Hereafter, all analyzed samples from this study are labeled according to the maximum temperature (in Celsius) at which they were exposed. Thus, the $Pu(C_2O_4)_2•6(H_2O)$ starting material, which was not heated, is labeled **Pu-25**. Samples heated to 100, 220, 250, 350, and 450°C are labeled **Pu-100**, **Pu-220**, **Pu-250, Pu-350,** and **Pu-450**, respectively. The selected temperatures were derived from previously reported thermogravimetric data which indicated significant mass changes occur near these temperatures.[4] Each of these samples exhibited a unique color that was not well-described in previous literature; therefore, we have provided a photo demonstrating the color of each sample (Figure 2-1).

Raman and IR band positions for all measured samples are provided in Table 2-1. Band assignments were determined by comparison with vibrational spectra of related compounds.[4, 7] Acquisition and tabulation of these spectral bands are the most crucial aspect of our study, as these data can be used to assess the accuracy of previously published DFT-derived intermediate structures associated with the Pu(IV) oxalate method.[6a]

Figures Figure 2-2, Figure 2-3, and Figure 2-4 present all pXRD, Raman, and IR measurements. Extensive descriptions on these data are presented in our recently submitted manuscript. The key features of these data that can be summarized as follows:

- Crystalline Pu(IV) oxalate hexahydrate ($Pu(C_2O_4)_2•6H_2O$) is the chemical species formed when oxalic acid is mixed with an acidic Pu(IV) nitrate solution; a result clearly established by all of our analytical measurements.
- $Pu(C_2O_4)_2•6H_2O$ has a rich vibrational spectrum with at least 15 Raman and 9 infrared bands between 180 – 2400 cm^{-1}.
- As $Pu(C_2O_4)_2•6H_2O$ is heated to 100 °C, water is liberated to produce crystalline $Pu(C_2O_4)_2•2H_2O$, which also has a rich vibrational spectrum.

- As $Pu(C_2O_4)_2 \cdot 2H_2O$ is heated above 100 °C, the oxalate ligand decomposes to produce amorphous plutonium oxycarbide species and ultimately yielding crystalline PuO_2 with some residual carbon-containing species when heated to 450 °C
- Small amounts of PuO_2 were found at calcination temperatures as low as 220 – 250°C. Observation of this result was aided by the ultra-sensitivity of Raman spectroscopy to the T_{2g} band of PuO_2 and the observation of the electronic band at 2640 cm^{-1}. The PuO_2 which forms near 220 – 250 °C appear to be nanoparticulates and future studies into the morphology of these nanoparticulates may prove useful to the Nuclear Forensics community. We are unaware of any previous evidence showing PuO_2 formation at such low temperatures.

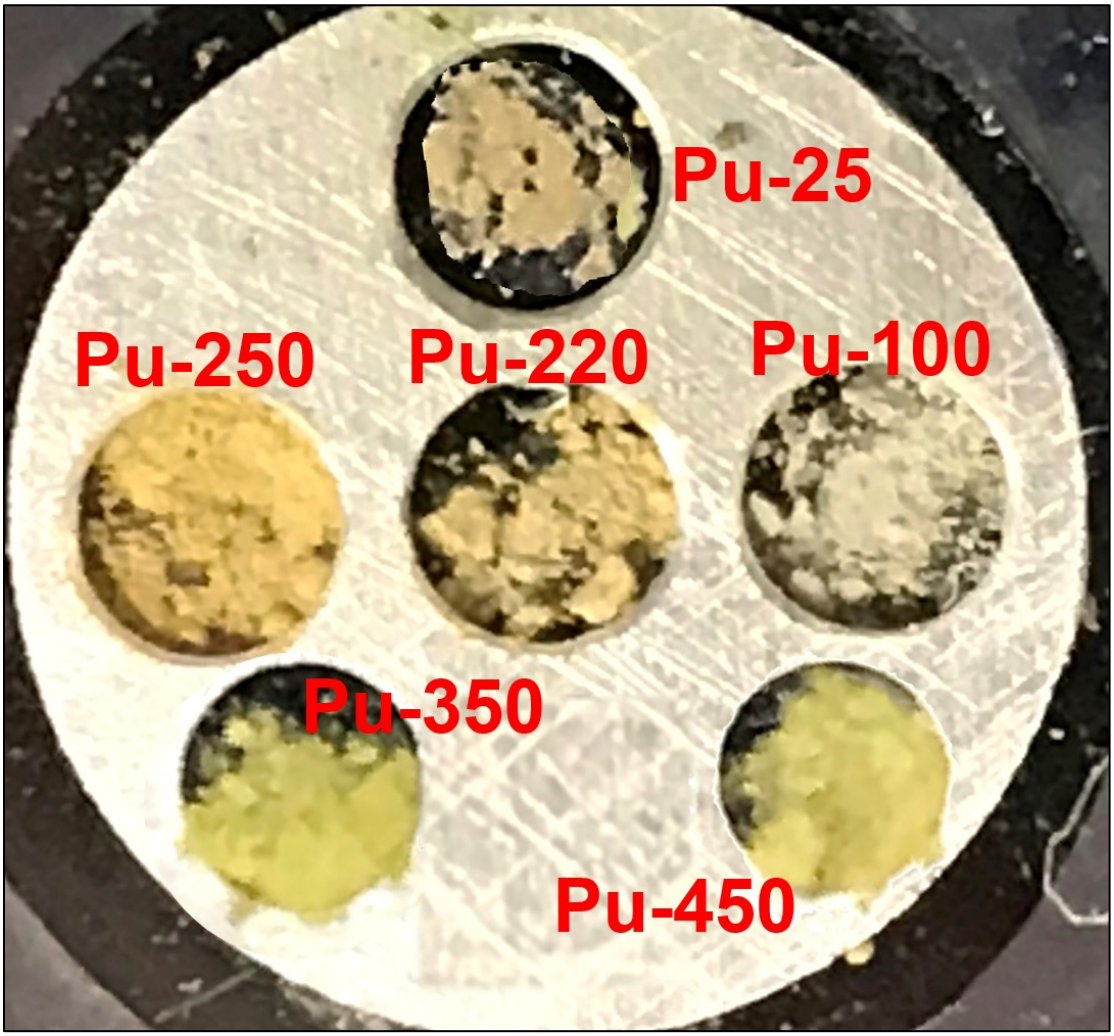

Figure 2-1. Visual appearance of $Pu(C_2O_4)_2 \cdot 6(H_2O)$ produced at room temperature **(Pu-25)** and its degradation products up to 450°C (**Pu-450**).

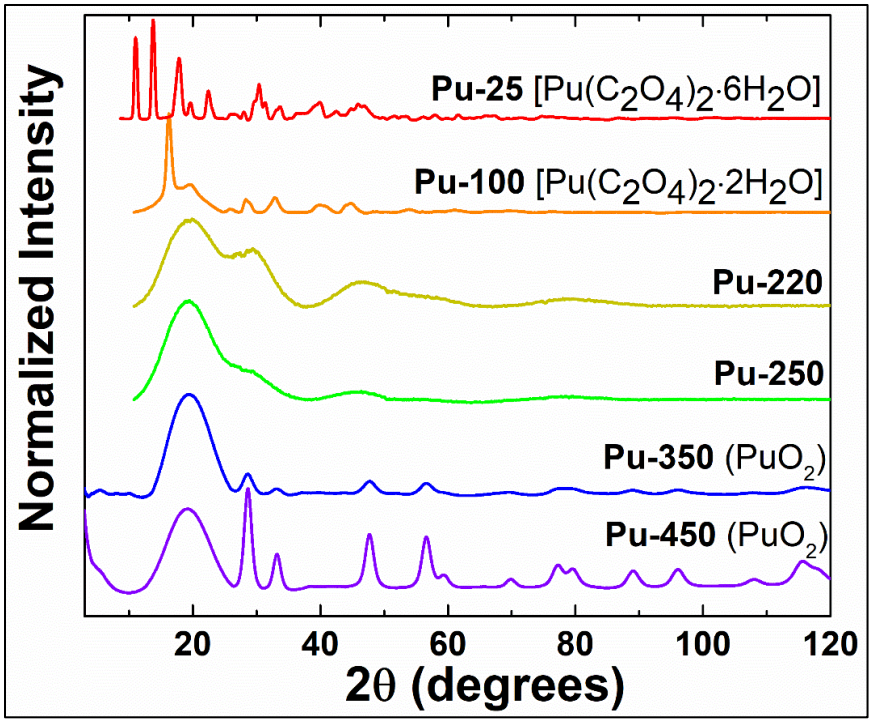

Figure 2-2. pXRD patterns of $Pu(C_2O_4)_2$•$6(H_2O)$ produced at room temperature (Pu-25) and its degradation products as it is heated to 450 °C (Pu-450).

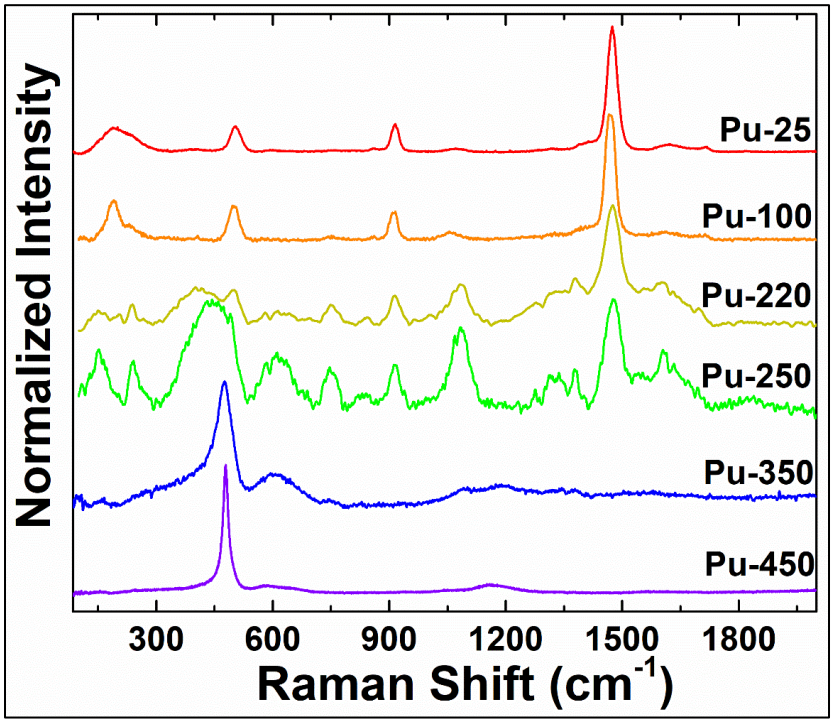

Figure 2-3. Raman spectra of $Pu(C_2O_4)_2$•$6(H_2O)$ produced at room temperature (Pu-25) and its degradation products as it is heated to 450 °C (Pu-450).

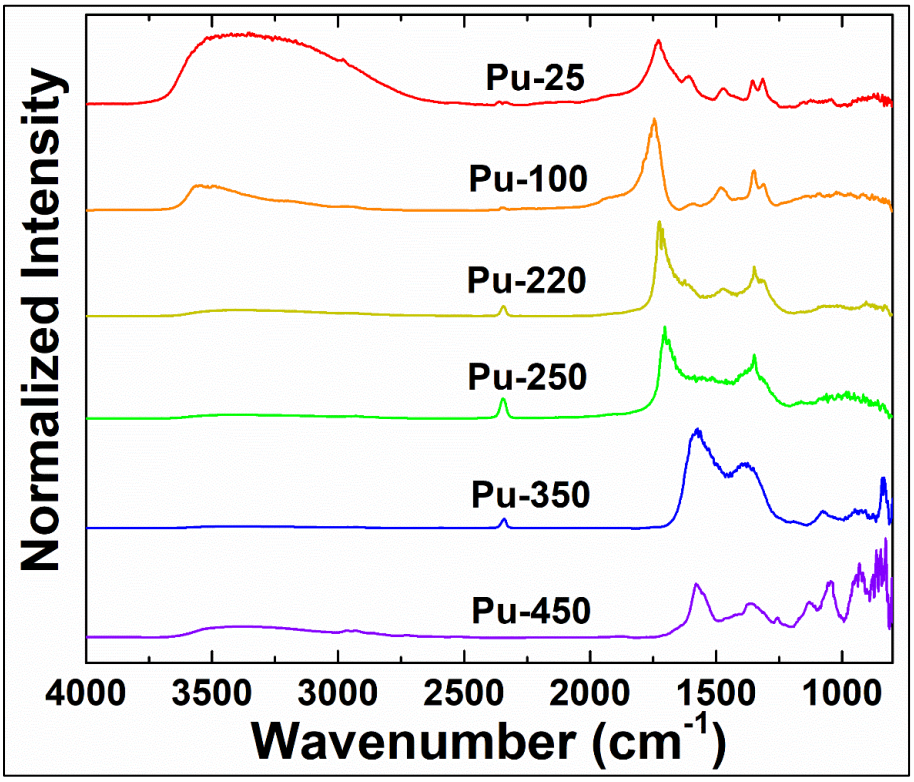

Figure 2-4. IR spectra of $Pu(C_2O_4)_2 \cdot 6(H_2O)$ (Pu-25) and its degradation products as it is heated to 450 ºC (i.e., Pu-450).

Table 2-1. Band positions for the vibrational spectra of Pu(IV) oxalate produced at room temperature (Pu-25) and its degradation products when heated up to 450ºC (Pu-450); band positions in cm^{-1}. Bands of similar wavenumbers are compiled in the same row. When practical, band assignments are listed and are based on comparison with related compounds; bands that could not be unambiguously assigned are not labeled.[4, 7a, 7b]

Pu-25		**Pu-100**		**Pu-220**		**Pu-250**		**Pu-350**		**Pu-450**		**Approximate vibrational mode assignments**
IR	*Raman*	*IR*	*Raman*	*IR*	*Raman*	*IR*	*Raman*	*IR*	*Raman*	*IR*	*Raman*	
	187		187									Pu-O and lattice
	241		241		241		241					Pu-O and lattice
	399		409		409		428					Pu-O and lattice
					481		481		474		478	T_{2g} of PuO_2
												δ(OCO)
	504		504									
									581		581	1LO2 of PuO_2
					604		604		604		604	Defect band of PuO_2
	754		754		754		754					
										802		
								820		827		
								833		847		
876	858		863		846		833	841				
										863		
										879		
												ν(C-C) +
1052	912	976	912	900	916	960	916	935		935		ν(CO) + δ(OCO)
	1070		1063									
										1049		
1120				1037		1161		1075		1131		
				828	1088		1088					ν(CO_3)
									1163		1163	2LO2 of PuO_2
1314	1319	1311		1313	1282		1278			1256		ν(CO) + δ(OCO)
1355		1350		1350	1333	1348	1333					ν(CO) + ν(C-C)
	1388		1388		1382		1382	1386		1362		ν(CO)
	1410		1410									
1471	1472	1480	1472	1474	1478		1480					ν(CO)
								1574		1579		
1606	1620	1590	1611	1621	1606		1608					ν(RCO_2) + ν(RCO)
1728	1715	1745	1715	1711		1702		1742				ν(C=O)
	1818									1880		
1920		1906		1906		1921		1925				
								2156				
								2276				
		2343		2343		2344		2340				ν(CO_2)
Multiple broad bands between 2400 – 3800												ν(OH) + ν(C-H)$_{contamination}$

2.2 Plutonium (IV) Fluoride Hydrate

2.2.1 Background

Pyrochemical preparation of plutonium metal is often carried out by reduction of PuF_4 or a mixture of PuO_2 and PuF_4 in molten salt as shown in equations **2** and **3**, respectively. Some processes utilize PuF_3 as an intermediate leading to PuF_4 and PuO_2 as shown in equation **4**. Anhydrous plutonium fluoride is typically prepared via high temperature fluorination of plutonium dioxide or oxalates using HF gas. When prepared using aqueous methods, PuF_4 and PuF_3 are said to assume hydrated forms of $PuF_4 \bullet 2.5(H_2O)$ and $PuF_3 \bullet 0.75H_2O$. Lattice water and plutonium fluorides are both prone to radiolysis from plutonium alpha emissions. The kinetics of PuF_4 and PuF_3 radiolysis and the degradation products formed during radiolysis are not currently known. Given its extensive use in the fuel cycle, characterization of radiolytic changes to these fluorides would be an important accomplishment that could provide information about time and method of production as well as proliferation risks

$$PuF_4 + 2Ca^0 \longrightarrow Pu^0 + 2CaF_2 \quad \textbf{(2)}$$

$$PuF_4 + PuO_2 + 2Ca^0 \longrightarrow 2Pu^0 + 2CaF_2 + O_2 \quad \textbf{(3)}$$

$$4PuF_3 + O_2 \rightleftharpoons 3PuF_4 + PuO_2 \quad \textbf{(4)}$$

2.2.2 Synthesis of Hydrated PuF_4

At the end of FY20, SRNL produced ~100 mg of hydrated plutonium fluoride using the following method.

21.5 mL of the purified 0.1 M $Pu(NO_3)_4$ solution was added to a 100 mL polypropylene beaker along with a magnetic stir bar. The solution was stirred at ~300 revolutions per minute and was maintained at ~ 25 °C using a heating/stir plate. 9 mL of 1 M HF was carefully added to the solution at a rate of ~3 mL/min using a calibrated positive displacement pump. Immediately following HF addition, the plutonium solution became cloudy and formed a pale pink precipitate that was consistent in appearance with plutonium tetrafluoride hydrate.[8]

The precipitate was filtered and dried under a flow of argon gas for approximately 24 hours. The dried pale pink solids were then collected and isolated in an argon atmosphere to minimize exposure to oxygen and ambient humidity.

Approximately 100 mg of these solids were carefully removed from the radiological glovebox for powder X-ray diffraction analysis of purity and chemical phase. Less than 1 mg of solids were carefully mounted to carbon adhesive tape inside a spectroscopy double-containment cell. The cell was then sealed in an argon environment, removed from the radiological glovebox with assistance from the SRNL Radiation Protection Department, and was delivered to the SRNL Laser Lab for characterization by both DRIFTS and Raman spectroscopy.

2.2.3 Characterization Results

As shown in Figure 2-5, the pXRD pattern for hydrated plutonium fluoride was consistent with the literature pattern for hydrated plutonium (IV) fluoride (PDF 00-034-0515). In general, this compound exhibited very weak diffraction peaks.

Micro-Raman spectra of the PuF_4 hydrate were acquired with a LabRAM HR800 UV (Horiba Jobin-Yvon) equipped with an Andor detector (DU146A-LDC-DD) with fringe suppression technology. Four excitation laser wavelengths (458, 488, 514, and 633 nm) were used to help distinguish vibrational modes from fluorescence since fluorescence will vanish when the laser excitation wavelength is changed but the Raman spectral signatures will not.

Similar to the fluorescence observed from UF_4 and the UF_4 hydrates[9], our sample exhibited fluorescence when exposed to each 457, 488, and 514 nm laser wavelengths (Figure 2-6). Although these spectra have not been calibrated for the instrument response, the spectra maxima are located around 600 nm and both the fluorescence and Raman spectra for our sample are very weak in intensity.

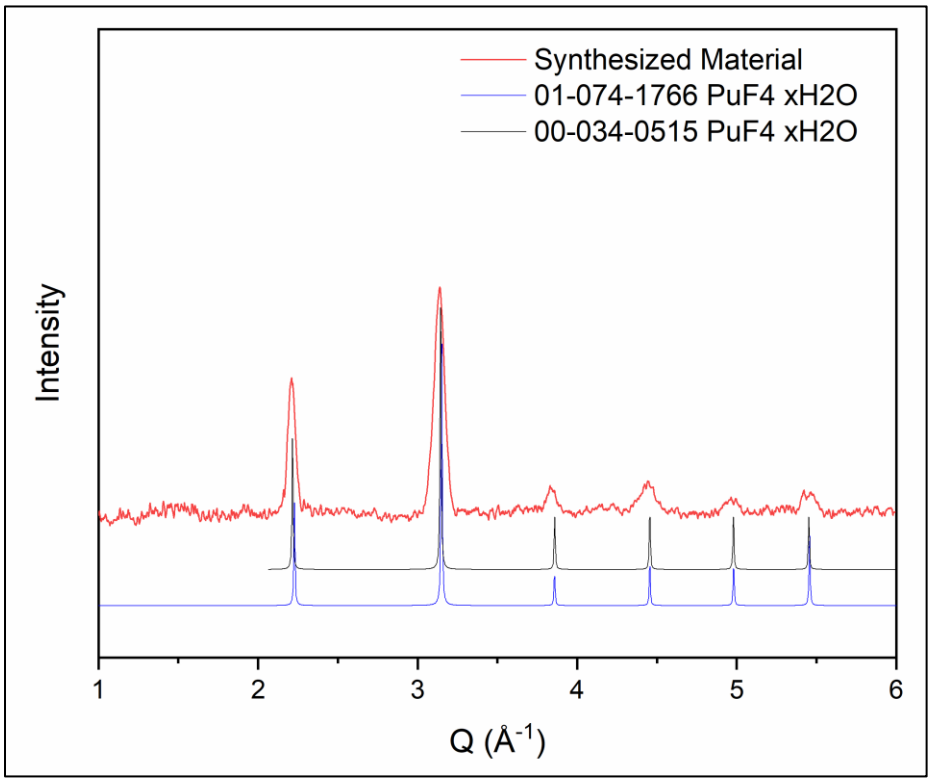

Figure 2-5. The PDF pattern of hydrated PuF_4 is displayed with the experimental pXRD pattern for hydrated PuF_4 solids obtained in our experiments.

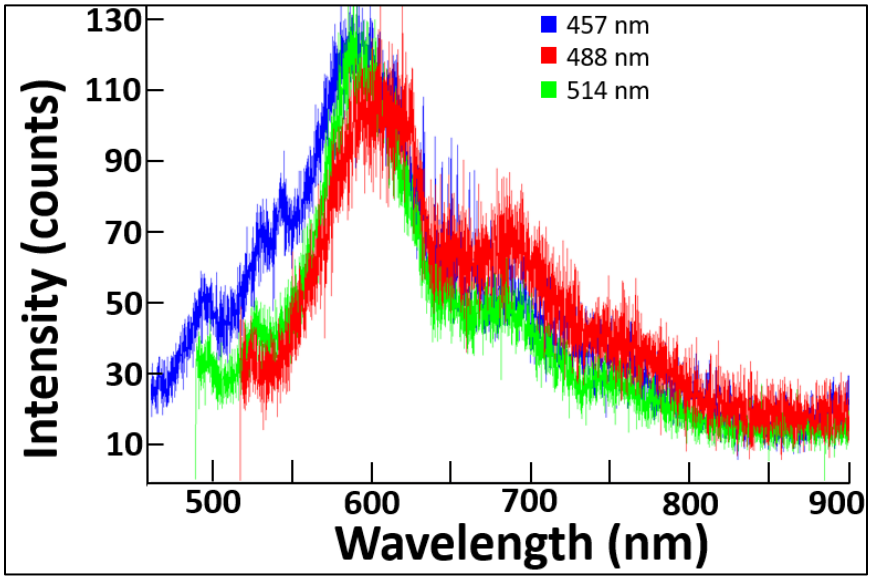

Figure 2-6. Fluorescence spectra of hydrated PuF_4 at various excitation laser wavelengths.

Close to the laser excitation wavelength, bands of very weak intensity were observed at 187, 241, 348, 403, 474, and 567 cm^{-1}. These bands were observed on a rising background toward the laser excitation line and were reproducible at different wavelengths, indicating they did not originate from sample fluorescence. Figure 7 shows these bands acquired at 488 and 633 nm laser wavelengths.

The source of the rising background seen in the spectra in Figure 2-7 does not seem to be fluorescence from PuF_4 since it persists across multiple laser excitation wavelengths. Instead, the rising background is likely due to a significant number of low-frequency modes from F-F polymeric interactions and the hydrogen bonding from water in the system. Importantly, after examining the spectra of several metal tetrafluoride compounds (ZrF_4, HfF_4, and CeF_4) in 1975, Goldstein *et al.*[10] postulated these compounds have a three-dimensional polymeric structure instead of the simplistic tetrahedral structure originally theorized by Krasser *et al.*[11] Although Goldstein *et al.* were unsuccessful in measuring the UF_4 Raman spectrum due to material decomposition, Villa-Aleman and Wellons successfully measured the spectrum in 2016[9] to confirm Goldstein's argument of a three-dimensional polymeric structure for some metal tetrafluorides, like UF_4. Based on the spectra in Figure 2-7, specifically the rising background, we suspect that PuF_4 has a similar polymeric structure; however, further studies with higher resolution are still needed to confirm this hypothesis.

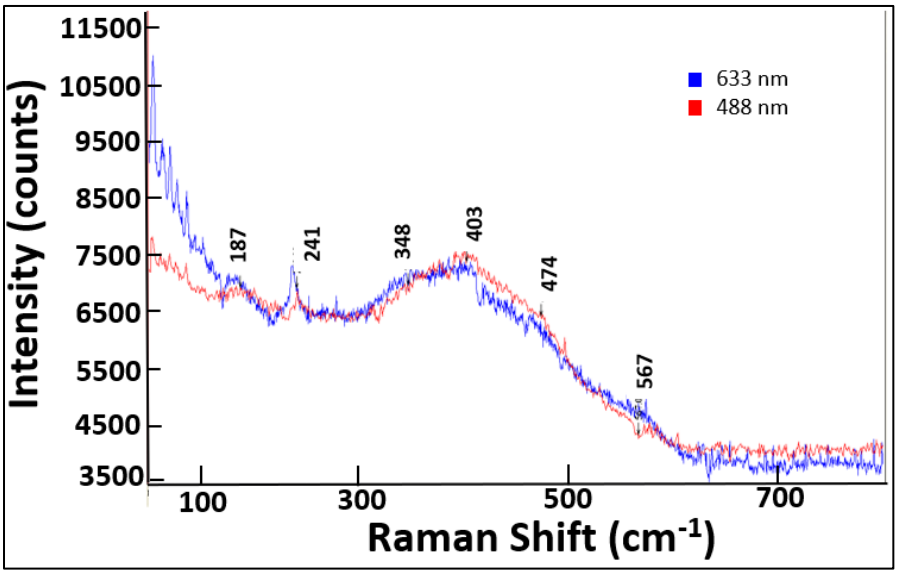

Figure 2-7. Raman spectra of hydrated PuF_4 when interrogated with a 633 and 488 nm excitation laser.

An issue with collecting high-fidelity Raman spectra on hydrated PuF_4 is that the intensity of the resultant Raman bands is extremely low and very few bands are observed (as compared to the Raman spectrum of UF_4). We postulated that this was due to low crystallinity of the material. The solubility of PuF_4 is extremely low in water, and the material immediately precipitates from solution once a fluoride source is added. Rapid precipitation such as this likely precludes crystallite growth yielding amorphous or weakly crystalline powders. In an effort to improve crystallinity, we annealed the sample at 200 °C and repeated Raman and pXRD measurements. Unfortunately, the material appeared unchanged by the annealing process.

To better understand the thermal stability of this material, we performed multiple thermogravimetric analysis (TGA) measurements. As shown in Figure 2-8, a total mass loss of ~6.54 wt.% was observed when the material was heated to 800 ºC in argon. Post-TGA pXRD showed that the final product after heating to 800 °C was PuF_3 (Figure 2-9). In summary, attempts to produce anhydrous PuF_4 or larger crystallites of hydrated PuF_4 by heating hydrated PuF_4 were unsuccessful and heating hydrated PuF_4 eventually leads to conversion to PuF_3.

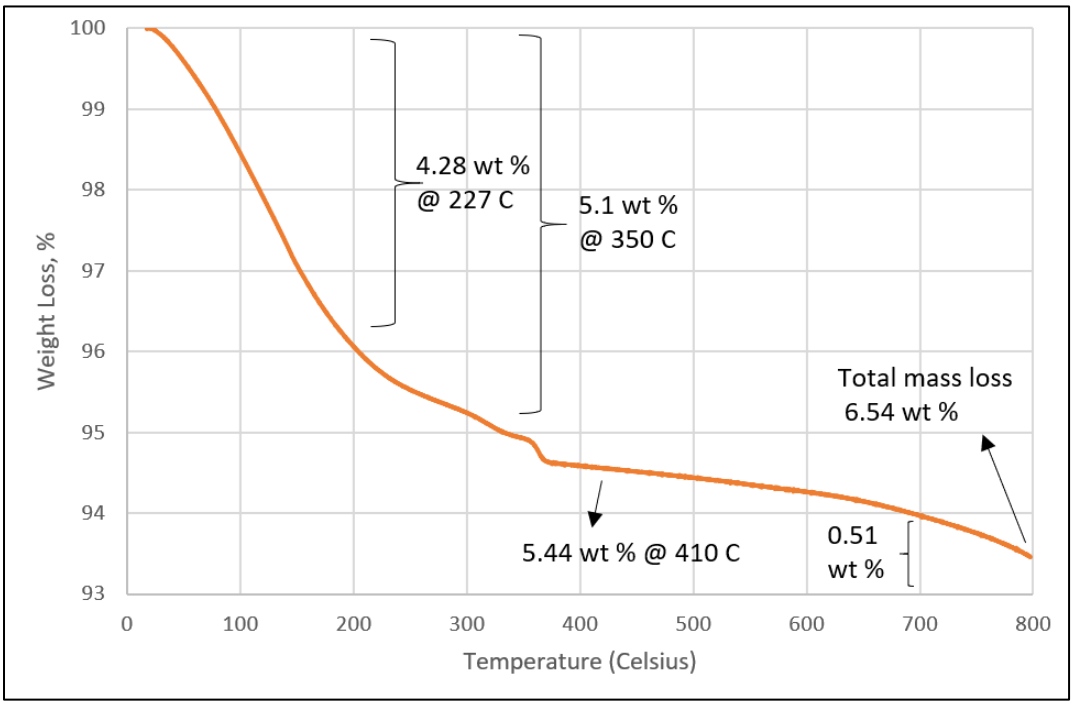

Figure 2-8. TGA data of hydrated PuF_4 analyzed under an argon atmosphere

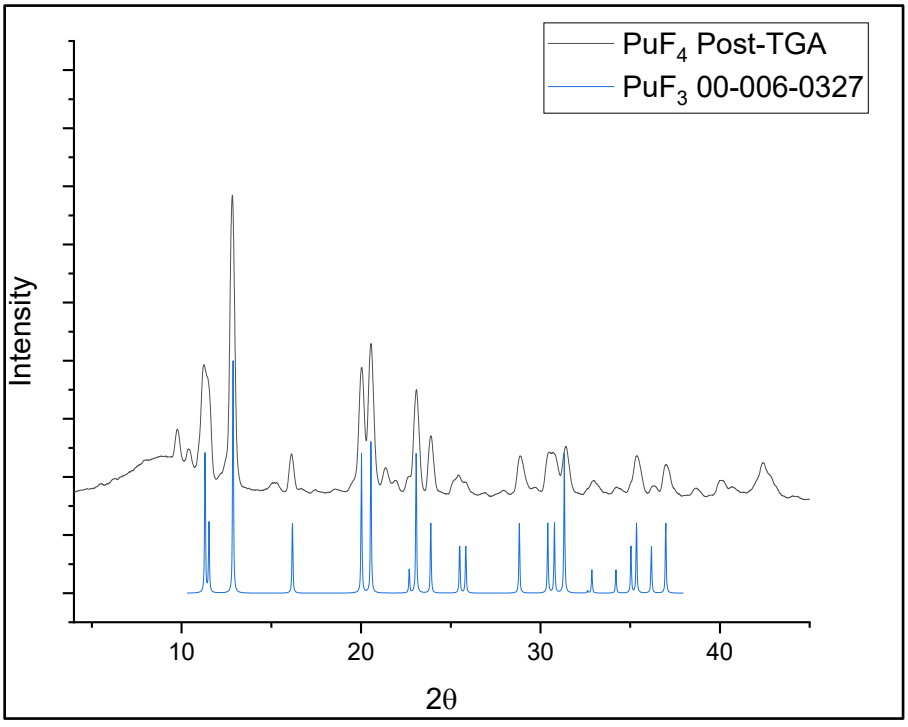

Figure 2-9. Powder on SC-XRD pattern for post-TGA material (black trace), which is consistent with the PDF card for PuF_3 (blue trace).

To confirm our suspicion that crystallite size is extremely small in precipitated PuF_4 hydrate, we measured the size of the precipitate with scanning electron microscopy (SEM). As shown in Figure 2-10, the solids formed by precipitation of PuF_4 hydrate are indeed extremely small. Thus, we can conclude the precipitation of PuF_4 hydrate occurs too fast to produce a highly crystalline material that would be amenable

towards advanced spectroscopic characterization. Efforts to increase crystallite size via thermal annealing proved unsuccessful up to 200 °C, and efforts are currently on-going to grow larger crystallites in solution.

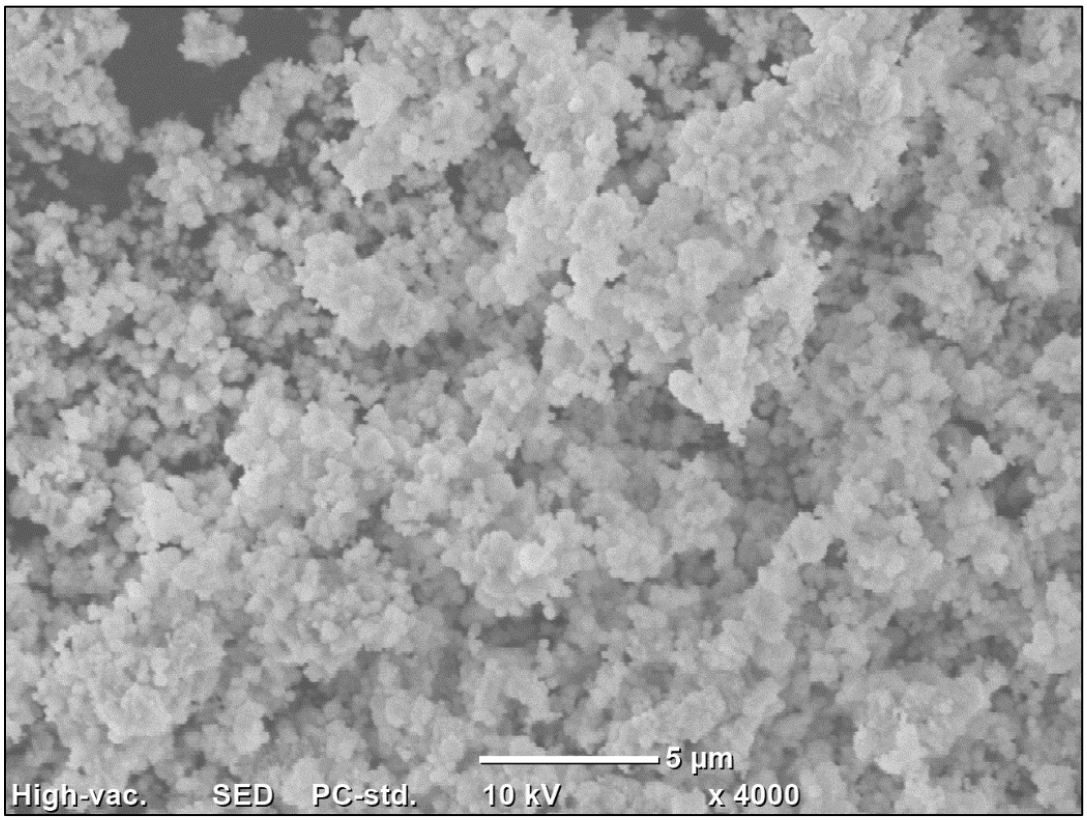

Figure 2-10. SEM micrographs of precipitated PuF_4 hydrate show the material consists of extremely small particulates.

Recognizing the difficulty in producing quality samples of PuF_4 and PuF_4 hydrate, the University of Notre Dame team began investigating novel synthetic techniques for producing these materials as described below in Section 2.3

2.3 Novel Synthesis Techniques for Producing Actinide Fluoride Samples

2.3.1 Background

Anhydrous actinide fluoride materials are typically prepared via high temperature fluorination of actinide oxides or oxalates using HF gas. Unfortunately, high temperature fluorination poses a number of safety hazards and is largely prohibited in many research facilities. This means that high quality samples of actinide fluorides can be difficult to acquire. In fact, the only recent paper published on PuF_4 appeared in 2017 from McCoy *et al*. at PNNL.[12] The sample used by this team was a forty year old PuF_4 sealed source that was used in the Plutonium Finishing Plant from 1970 – 2010. Although PuF_4 can be prepared by fluoride precipitation from aqueous solution, synthesis of a high-fidelity, crystalline sample of PuF_4 in this fashion poses several scientific challenges (as described in Section 2.2).

Recently, new synthetic methods have appeared in the literature for producing UF_4 without high temperature corrosive gas.[13] Recognizing the possible utility of these methods to produce high quality PuF_4 specimens that would be amenable towards subsequent characterization studies, our team attempted to adapt these synthetic methods to Pu. These experiments occurred at the University of Notre Dame and were mainly performed with CeO_2 and UO_2 as surrogates for PuO_2 in FY21. This surrogate work allowed our team to develop robust procedures for handling fluorinated actinides prior to manipulating radioactive Pu samples.

2.3.2 Attempted Synthesis of Anhydrous CeF_4 (PuF_4 surrogate) with XeF_2

Attempts to synthesize anhydrous CeF_4 were performed following the approach by Inabinett et al. (i.e., fluorination using XeF_2).[13a] Briefly, excess molar ratios of CeO_2 and XeF_2 were placed in a perfluoroalkoxy (PFA) vial under nitrogen atmosphere in a negative-pressure glovebox. The vial was transferred to a Parr reaction vessel and was heated for varying lengths of time (5–24 hrs) and at varying temperatures (≤ 205 °C).

2.3.3 Successful Synthesis of Anhydrous UF_4 with an Ionic Liquid

Anhydrous UF_4 was synthesized following the approach reported by Florian et al. (2020), which uses the ionic liquid 1-Butyl-3-methylimidazolium hexafluorophosphate, [BMIM][PF6].[13b] For the synthesis, 40 mg of UO_2 and 2 ml of [BMIM][PF6] were placed in a Teflon reactor under nitrogen in a negative-pressure glovebox. The reactor was then placed in a Parr reaction vessel and heated at 180 °C for 96 hours. The green powder of UF_4 was noticeable upon centrifugation and after washing with CH_2Cl_2. Powder X-ray diffraction by single crystal matches perfectly with the powder patterns reported Florian et al. (2020) and with PDF card # 01-082-2317 (anhydrous UF_4). Thermal gravimetric analysis (TGA) confirms UF_4 to be anhydrous. To meet the three layers of containment necessary for Pu, a recent UF_4 synthesis attempting the use of perfluoroalkoxy (PFA) vials in a Parr reaction vessel with no water has also proven to be successful.

2.3.4 Results

As described above, numerous synthesis experiments were attempted using CeO_2 and XeF_2. Thus far, we hypothesize that the quarter inch of water necessary for Parr reaction vessels to interact with the starting material results in the formation of $CeF_4 \cdot 0.9H_2O$ with minor side products. To avoid hydration of the material, alternative closed systems, such as glass ampules and Swagelok tubes, were explored. Powders from glass ampules resulted in CeF_3 and a mixed phase of starting material with CeF_3. Synthesis attempts involving Swagelok tubes resulted no change to the starting materials.

The most promising results from these experiments so far were achieved when XeF_2 was mixed and heated with CeO_2 at a 6:1 ratio at 130 °C for 10 hours (Figure 2-11) and a 5:1 ratio at 150 °C for 10 hours (Figure 2-12). In both cases, the dominant chemical phases appear to be CeF_4 and CeF_3 although some byproducts (hydrates and CeO_2) persist. Notably, CeO_2 appears to be absent from the pXRD pattern resulting from the 5:1 XeF_2:CeO_2 reaction. University of Notre Dame will continue experiments with XeF_2 in FY22.

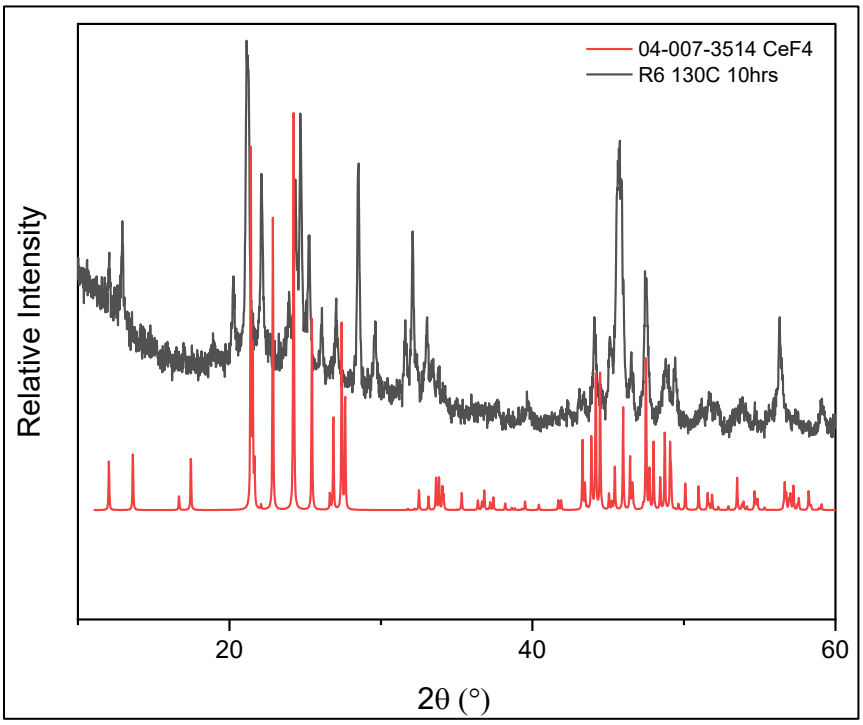

Figure 2-11. (Black) pXRD patterns for solids obtained after mixing XeF_2 and CeO_2 (6:1 ratio) for 10 hours at 130 °C. (Red) The database PDF pattern for CeF_4 (04-007-3514).

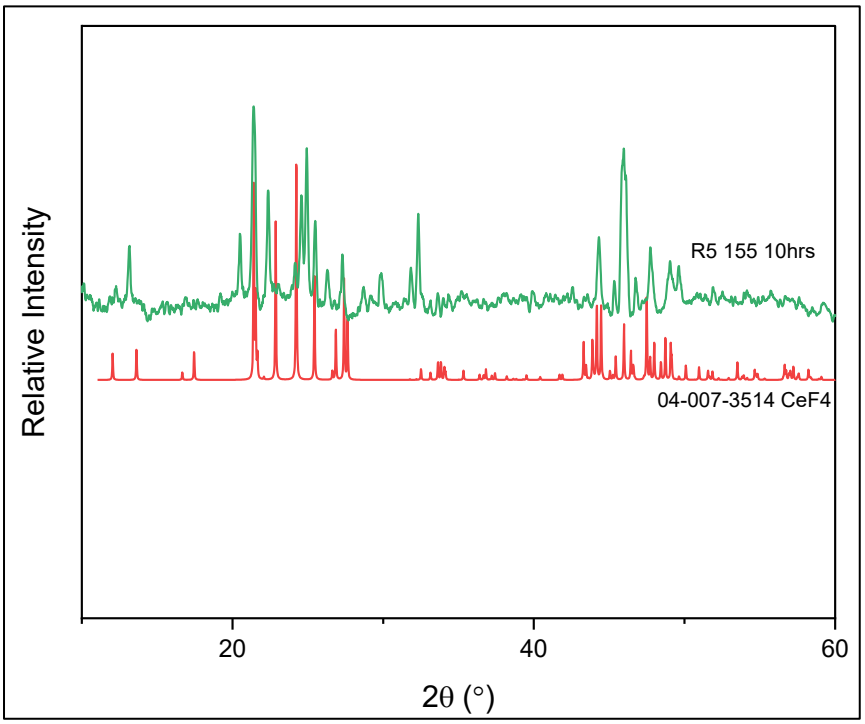

Figure 2-12. (Green trace) pXRD of solids obtained after mixing XeF_2 and CeO_2 (5:1 ratio) for 10 hours at 155 °C. (Red trace) The database PDF pattern for CeF_4 (04-007-3514)

A significant accomplishment by the Notre Dame team was the successful synthesis of anhydrous UF_4 using the ionic liquid [Bmim][PF6].[13b] In FY22, UND will attempt to adapt this method to cerium and plutonium. If successful, we expect the production of high quality PuF_4 to have a major impact on our future efforts to characterize nuclear fuel cycle materials. In fact, there are at least two dozen publications in the literature pertaining UF_4 and we propose that many of these studies could be reproduced with PuF_4.

2.4 $Pu(NO_3)_4$

2.4.1 Background

The majority of liquid-based plutonium processing operations occur in nitric acid. Thus, plutonium nitrate is a major component used in the nuclear fuel cycle.

2.4.2 Synthesis of $Pu(NO_3)_4$

Weapons-grade (~93% Pu-239) plutonium dioxide (PuO_2) was heated for several hours at ~100 °C in a mixture of 8 M nitric acid and a minimal amount (~0.5 M) of sodium fluoride to afford dissolution of the material. This solution was purified using an anion exchange column loaded with a commercial, positively charged, quaternary amine strong base resin, Reillex HPQ. The column was rinsed twice with 8 M nitric acid before introducing the 8 M plutonium nitrate solution. When dissolved in HNO_3 (between 7 – 9 M), plutonium is primarily in the hexanitrato form, $Pu(NO3)_6^{2-}$, which has a high affinity for the Reillex HPQ resin. Most other elements do not form stable anionic complexes at such high nitric acid concentrations and as such have very little affinity for resin. Purified plutonium nitrate, $Pu(NO_3)_4$, was eluted using dilute ($\leq$ 1 M) nitric acid.

The eluted solution was adjusted to ~1 M HNO_3 and was analyzed for plutonium concentration using gamma spectroscopy. The plutonium concentration was measured as ~0.1 M.

A 1 mL aliquot of the purified $Pu(NO_3)_4$ solution was added to a vacuum flask and was dried under reduced pressure for approximately 5 hours. The resultant product was a green, sludge-like substance that was then further dried under argon to produce solid $Pu(NO_3)_4$.

2.4.3 Results

Raman measurements of $Pu(NO_3)_4$ were quite rich, showing at least a dozen bands between 100 cm^{-1} and 2000 cm^{-1} (Figure 2-13). Additional characterization of this material along with assigning bands is scheduled for FY22.

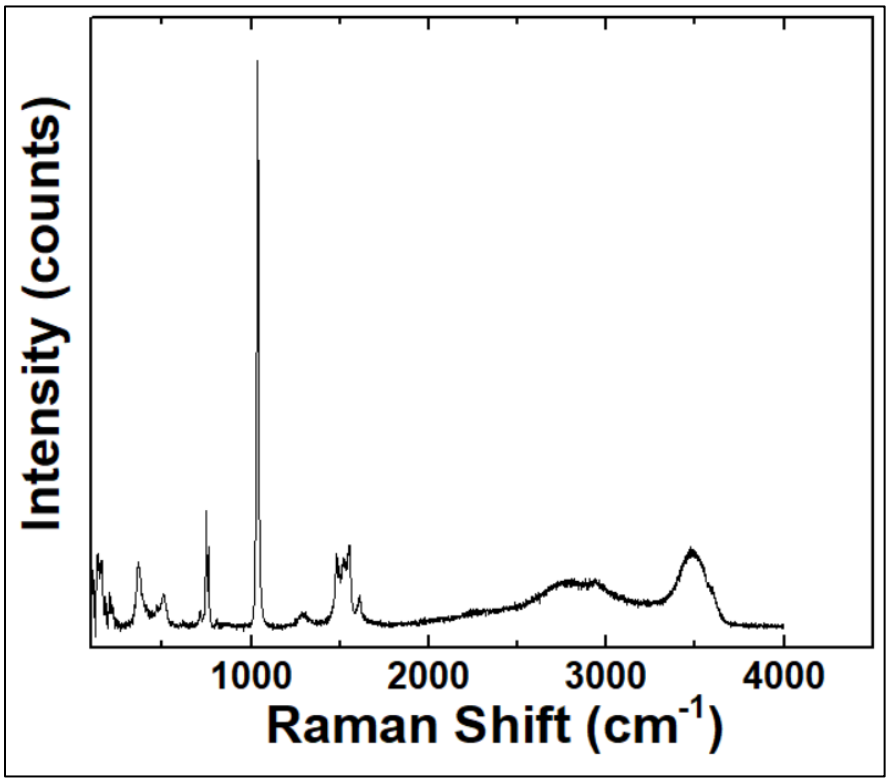

Figure 2-13. Raman spectrum of solid $Pu(NO_3)_4$.

3.0 Conclusions

In FY21, SRNL and UND engaged in numerous research studies involving production and subsequent characterization of plutonium dioxide, plutonium fluoride, plutonium oxalate, and plutonium nitrate. Vibrational spectroscopy, microscopy, X-ray diffraction, and thermogravimetric analysis were used to explore the spectroscopic, structural, and chemical properties of these plutonium compounds. Although largely fundamental in nature, the results presented herein shine new light on the properties of many of these compounds and should have utility in improving plutonium nonproliferation efforts.

4.0 References

1. Wick, O. J., *Plutonium Handbook: A Guide to the Technology*. American Nucear Society: La Grange Park, IL, 1980.
2. Patterson, J. P.; Parkes, P., *Recycling uranium and plutonium*. Oxford University Press: United Kingdom, 1996.
3. (a) Jenkins, I. L., Moore, F. H., Waterman, M. J., *Chem. and Indus.* **1963,** *35*; (b) Jenkins, I. L.; Waterman, M. J., The thermal decomposition of hydrated plutonium(IV) oxalates. *Journal of Inorganic and Nuclear Chemistry* **1964,** *26* (1), 131-137.
4. Vigier, N.; Grandjean, S.; Arab-Chapelet, B.; Abraham, F., Reaction mechanisms of the thermal conversion of Pu(IV) oxalate into plutonium oxide. *Journal of Alloys and Compounds* **2007,** *444-445*, 594-597.
5. Cleveland, J. M., *Section IV: Chemical Processing in Plutonium Handbook: A Guide to the Technology*. LaGrange Park, IL: American Nuclear Society, 1980; Vol. 2.
6. (a) South, C. J.; Roy, L. E., Insights into the thermal decomposition of plutonium(IV) oxalate – a DFT study of the intermediate structures. *Journal of Nuclear Materials* **2021,** *549*, 152864; (b) Garrett, K. E.; Ritzmann, A. M.; Smith, F. N.; Kessler, S. H.; Devanathan, R.; Henson, N. J.; Abrecht, D. G., First principles investigation of the structural and bonding properties of hydrated actinide (IV) oxalates, An(C2O4)2·6H2O (An = U, Pu). *Computational Materials Science* **2018,** *153*, 146-152; (c) Abraham, F.; Arab-Chapelet, B.; Rivenet, M.; Tamain, C.; Grandjean, S., Actinide oxalates, solid state structures and applications. *Coordination Chemistry Reviews* **2014,** *266-267*, 28-68.
7. (a) Nakamoto, K., *Infrared and Raman Spectra of Inorganic and Coordination Compounds - Application in Coordination, Organometallic, and Bioinorganic Chemistry*. Wiley: Hoboken, NJ, 2009; (b) Desfougeres, L.; Welcomme, É.; Ollivier, M.; Martin, P. M.; Hennuyer, J.; Hunault, M. O. J. Y.; Podor, R.; Clavier, N.; Favergeon, L., Oxidation as an Early Stage in the Multistep Thermal Decomposition of Uranium(IV) Oxalate into U3O8. *Inorganic Chemistry* **2020,** *59* (12), 8589-8602; (c) Frost, R. L.; Weier, M. L., Raman spectroscopy of natural oxalates at 298 and 77 K. *Journal of Raman Spectroscopy* **2003,** *34* (10), 776-785.
8. Clark, D. L.; Hecker, S. S.; Jarvinen, G. D.; Neu, M. P., *The Chemistry of the Actinide and Transactinide Elements*. 3rd ed.; Springer, Dordecht, 2010.
9. Villa-Aleman, E.; Wellons, M. S., Characterization of uranium tetrafluoride (UF4) with Raman spectroscopy. *Journal of Raman Spectroscopy* **2016,** *47* (7), 865-870.
10. Goldstein, M.; Hughes, R. J.; Unsworth, W. D., Spectrochim. Acta, Part A. 1975, 31A, 621. *Spectrochim. Acta, Part A. 1975, 31A, 621.*
11. W. Krasser, H. W. Nuernberg, Spectrochim. Acta, Part A 1970, 26,
1059.
12. McCoy, K.; Casella, A.; Sinkov, S.; Sweet, L.; McNamara, B.; Delegard, C.; Jevremovic, T., Radiation damage and annealing in plutonium tetrafluoride. *Journal of Nuclear Materials* **2017,** *496*, 379-387.
13. (a) Inabinett, D.; Knight, T.; Adams, T.; Gray, J., Study of XeF2 fluorination potential against Rh2O3, RuO2, ZrO2, and U3O8 for use in reactive gas recycle of used nuclear fuel. *Progress in Nuclear Energy* **2014,** *76*, 106-111; (b) Joly, F.; Simon, P.; Trivelli, X.; Arab, M.; Morel, B.; Solari, P. L.; Paul, J.-F.; Moisy, P.; Volkringer, C., Direct conversion of uranium dioxide UO2 to uranium tetrafluoride UF4 using the fluorinated ionic liquid [Bmim][PF6]. *Dalton Transactions* **2020,** *49* (2), 274-278.